EUROPEAN ORGANIZATION FOR NUCLEAR RESEARCH
Laboratory for Particle Physics

Divisional Report

CERN LHC/2000-4 (MTA)
CERN-NuFACT Note 035

Response of Solid and Liquid Targets to High Power Proton Beams for Neutrino Factories

P. Sievers and P. Pugnat

Abstract

The response of solid and liquid targets to rapid heating by the incident proton beam is assessed in a classical way, among other things by solving the wave equation under linear conditions and in cylindrical symmetry. This study provides bench mark values and allows to identify critical issues and limiting factors which can help to guide further investigations with more sophisticated means.

Administrative Secretariat
LHC Division
CERN
CH - 1211 Geneva 23

Geneva, Switzerland
12 October 2000

1. Introduction

Among the main issues for pion production in solid or liquid targets for neutrino factories are the evacuation of the average power deposited by the intense proton beam incident on the target and the instantaneously (within a few nano-seconds) deposited energy leading to rapid temperature rises and stresses in the material. In this basic assessment the response of the target material to the rapid heating will be evaluated, assuming material constants independent of temperature and pressure. This study serves to identify relevant parameters and critical areas where non-linear effects become important and where more sophisticated methods and tools have to be applied.

2. Input Parameters

For the use of solid targets, Tantalum has been suggested (Ref. 1) and for liquid targets, mercury is proposed (Ref. 2). The constants used for both these materials are given in Annex I. Most of the results will, however be quoted in relative units, so that they can readily be scaled to targets with different material constants and dimensions.
For the proton beam an average power of 4 MW is considered, incident on the target in short energy pulses (bursts) of 80 kJ/burst each, at 50 Hz. A parabolic radial energy deposition density ρ is assumed, dropping to zero at the outer radius R = 1 cm and being uniform along the target:

$$\rho(\mathrm{r}) = \rho_0 \left[1 - (r/R)^2\right]$$

R = 1 cm

ρ_0 = 40 J/gr.

With this assumption about 25% of the incident energy remains in the considered Ta-target of 2 cm diameter and 20 cm length.

3. First Order Approximations

Converting the peak energy density per burst into an instantaneous temperature rise along the center of the target, yields:

ΔT_0 = 265 K for Ta

and ΔT_0 = 286 K for Hg.

Now, since the rise time of the temperature is of the same order of magnitude as the deposition of the beam energy, which is 10^{-9} s, thermal expansion is initially prevented by the mass inertia of the material. The resulting instantaneous stress ($\Delta\sigma$) and pressure (ΔP) rise at time t = 0 is given by:

$$\Delta\sigma(r) = \frac{E\alpha_L \, \Delta T(r)}{1 - 2\nu}$$ for a solid (all three principal stresses are equal)

and $\Delta P(r) = \dfrac{\alpha_V \, \Delta T(r)}{\kappa}$ for a liquid.

For the above parameters this yields along the center:

$\Delta\sigma_0 =$ 826 MPa for Ta

and $\Delta P_0 =$ 1150 MPa for Hg.

Assuming now linear elastic behaviour of the target, the instantaneously pressurized material will start to oscillate since at time zero it is not in its equilibrium position. This can readily be compared to a pendulum for which the location of its "equilibrium" suspension is instantaneously be shifted. If this shift occurs slower and within times comparable to the pendulum frequency, its oscillation amplitude will be smaller, and if this shift occurs very slowly it will not oscillate at all. The latter case corresponds to a "slow" heating with "quasi-static" thermal expansion.

Note that the response of material to rapid heating is different from that induced by the impact of a supersonic bullet which actually displaces material radially with supersonic velocity along its path. This would be equivalent to displacing the mass of the pendulum with supersonic speed which is different from displacing rapidly its equilibrium suspension.

For liquid targets it is relevant to assess the energy E_C stored in the material due to the initially prevented thermal expansion of the target as this might be converted into kinetic energy ripping the liquid apart. The energy density dE_c/dV is given by:

$$dE_c/dV = \frac{(\alpha_V \Delta T(r))^2}{2\kappa} \; .$$

By integration over the volume, the total energy E_C, convertible to velocity for the assumed Hg-target with a length of 25 cm is about

E_C = 780 J/pulse for Hg

and the "average" kinetic power, W_C to be handled in the vicinity around this "exploding" liquid is

W_C = 39 kW.

This is with the assumed parameters about 4 % of the total deposited power.

By inspecting the kinetic energy density dE_c/dV and its integral over the target volume it can be shown that with beams of normalized intensity the total kinetic energy E_C deposited in the target is proportional to the temperature rise ΔT_0 on the target axis. From this it results that E_C depends on the radius R of the normalized beam as $1/R^2$, i.e. E_C rises sharply with narrow beams.

The order of magnitude of the velocity with which the boundary of the liquid target material can explode in radial direction is simply given by the radial, thermal expansion at the boundary divided by the time over which the sound travels across the radius of the target:

$$\bar{v}/c \approx \alpha_V \Delta T_0 / 4$$

c: velocity of sound.

This estimate yields for the considered cases that the material velocities during oscillations or at explosion are only of the order of a percent of the sound velocity. As a consequence one may believe that supersonic shock phenomena are not yet relevant at the above-assumed parameters.

Still, the problem is unsolved whether the liquid will explode once the pressure turns to negative during its oscillation, rather than sustaining negative pressures and continuing to oscillate, as one may expect for solids.

The involved frequencies of the radial oscillations are of the order of

$$f_R = c/4R.$$

With the sound velocity of 3.8 km/s and 1.3 km/s for Ta and Hg respectively this yields

$$f_R \approx 95 \text{ kHz for Ta}$$

$$f_R \approx 32 \text{ kHz for Hg}$$

which is within the ultra-sound region.

4. Results

4.1 Solids

The linear response in space and time of mass material submitted to an initial stress or pressure distribution is described by the classical wave equation. In cylindrically symmetrical configuration, as can be assumed for the targets concerned, the wave equation can be solved with the appropriate initial and boundary conditions by a Fourier-Bessel series. In an early assessment this has been reported in Ref. 3 for longitudinally and radially constrained solids. The extension of this work to radially free solid and liquid targets is given in Ref. 4.

Solving the wave equation yields all relevant parameters, like radial, circumferential and axial stresses for solids and pressure and material velocities for liquids as function of radius and time (Ref. 4).

Here we quote only final results. Fig. 1 shows the equivalent von Mieses stress vs. time along the center of the rod and Fig. 2 gives the same at its free boundary. The stress is given in units of $E\alpha_L \Delta T_0$ and the time in units of R/c. This allows to use these plots for any material, dimension and temperature rise, however all with parabolic temperature distributions up to the outer radius R. It results that at t = 0, where all principal stress

components are equal (see chapter 2) and where the solid is simply put under "hydraulic" pressure, the equivalent stress is zero. Due to subsequent acceleration and displacements the equivalent stresses start to oscillate and a maximum of

$$1.8\,\mathrm{E}\alpha_{\mathrm{L}}\Delta T_0 = 496\ \mathrm{MPa}$$

is reached in the center of the Ta-rod after

$$1.4\,\mathrm{R/c} = 3.7\ \mu\mathrm{s}.$$

Thereafter it continues to oscillate in a nearly harmonic fashion with a frequency of about 130 kHz close to the estimated value given in chapter 3. At the boundary a maximum equivalent stress of

$$1.3\,\mathrm{E}\alpha_{\mathrm{L}}\Delta T_0 = 358\ \mathrm{MPa}$$

is reached. Both the values at the center and at the boundary are still within the elastic limit of Ta at room temperature. These results are in excellent agreement with those quoted in Ref. 1, which were achieved with the finite element code ANSYS. The response to such stresses occurring at 50 Hz and possibly at elevated temperature (due to slow cooling) has to be assessed further.

One may speculate that the peak stresses can be reduced by longer proton bunches where the heating occurs slower and where mass inertia effects are reduced. In Fig. 1 and Fig. 2 the equivalent stresses are also shown for continuous heating over longer duration θ_0 of $0.5, 1, 2$ and 10.

$$\theta_0 = \mathrm{c}\,\mathrm{t}_0/\mathrm{R}$$

$$\mathrm{t}_0 = \text{heating time.}$$

As however expected, this effect becomes significant only above $\theta_0 \approx 1$, corresponding to $\mathrm{t}_0 = 2.6\ \mu\mathrm{s}$ for Ta.

4.2 Liquids

In a similar fashion as for solids the wave equation has been solved for a radially free liquid with an initial, parabolic temperature and thus pressure distribution. Fig. 3 and Fig. 4 show the pressure and the material velocity respectively vs. radius at different times. The pressure is given in units of $\alpha_{\mathrm{V}}\Delta T_0/\kappa$, the velocity in units of $\mathrm{c}\ \alpha_{\mathrm{V}}T_0$, the radius in units of R and the time parameters in R/c. These plots are generally valid for any material constants with a parabolic energy deposition density. Fig. 5 and Fig. 6 show the pressure at r = 0 and the material velocity at r = R respectively vs. time. At times $\theta > 0.74$ ($t > 5.7$ μs for Hg) the pressure becomes negative, i.e. as of this instant cavitation (brake-up) of the liquid may occur and all subsequent pressure and velocity profiles are no longer valid. However, as can be seen in Fig. 6 the maximum velocity at the boundary is reached at the same time. Thus, in case of immediate cavitation for $P<0$ the material will fly off at the rim with a velocity of

$$\hat{\mathrm{v}}/\mathrm{c} = 0.54\,\alpha_{\mathrm{V}}\Delta T_0$$

or $\hat{v} = 36$ m/s for Hg,

which is double the value estimated in paragraph 3. This may be explained by the fact that there the average velocity is given while here the peak velocity is quoted.

For illustration, a Hg-droplet flying off vertically with this velocity will ideally reach a maximum height of 65 m.

Again the central pressure and the velocity at the boundary are reduced by extending the time of heating as illustrated in Fig. 5 and Fig. 6. As for solids this effect sets in only for durations of heating of $t_0 > 4\,\mu s$.

As can be seen from the above considerations the pressure and the material velocity both depend on the compressibility like

$$P \sim 1/\kappa \quad \text{and} \quad v \sim 1/\sqrt{\kappa}$$

Thus increasing the compressibility would have a beneficial effect. Indeed, liquid metals "loaded" with bubbles or liquid jets made of micro-droplets have been suggested which could substantially change the response of liquid targets modified in such a way.

4.3 Damping of oscillations inside a 20 T solenoid

As one can see from Fig. 6 the material at the boundary of the target moves radially similar to a harmonic oscillator. Since it is envisaged to place the Hg-target inside a solenoid with an axial magnetic field of 20 T one can estimate the change of the oscillation, associating it with an oscillator, magnetically damped by a term proportional to its velocity. The damping time δ is

$$\delta = 2\,\rho/\varepsilon\, B_z^2 .$$

ε : Electrical conductivity of Hg
B_z : Field of the solenoid, 20 T
ρ : Density of Hg

Putting in the numbers, this yields:

$$\delta \approx 67\ \mu s.$$

Since this is large compared to the time $t \approx 5.7\ \mu s$ to reach the first peak of velocity, damping can be neglected for the first oscillations, i.e. the velocities displayed in Fig. 6 over the first 20 μs will not be reduced significantly and, if the material brakes up at P<0 it will fly off at the velocity estimated above.
Still, these results must be considered as somewhat pessimistic, since nevertheless some internal friction and braking will occur due to surface tension and viscosity of the liquid. It may however be expected that these effects are even smaller than the magnetic friction.

5. Axial and Lateral Oscillations

Throughout the above considerations, axially constrained targets were assumed. In instantaneously heated cylinders, free at both ends, also axial relaxation waves will propagate from both ends towards the center with the velocity of sound.

Over the time the radial pressure wave has propagated from the boundary to the center, the axial wave has propagated by about the same distance, i.e. in our case 1 cm, from the free ends towards the center. Thus for long targets most of the central part can still be considered as axially constrained over many periods of radial oscillations. A good estimate for the axial stress resp. pressure is

$$\hat{\sigma}_z = \pm E\alpha_L T(r) \quad \text{for a solid}$$

and

$$\hat{P}_z = \pm \frac{\alpha_V T(r)}{\kappa} \quad \text{for a liquid.}$$

If the length heated by the proton beam is shorter than the actual target rod, like for the toroid, discussed in ref. 1, axial stress waves will propagate also into the adjacent, not heated zones. Moreover, long, slender solid rods put under axial stress may also respond to this load by buckling.

When by mis-stearing of the incident proton beam onto the target a temperature distribution is created which is not rotationally symmetric around the target axis, bending stresses, like in a bi-metal, will occur. The equilibrium shape of the target is "bent" while due to mass inertia the target is still straight at time zero. It will start to oscillate with its fundamental lateral frequency f_ℓ :

$$f_\ell = c_o \sqrt{I/B}\ \frac{\pi}{2L^2}$$

I : Moment of inertia
B : Cross-section area
L : Target length
c_o : Axial sound velocity $\sqrt{E/\rho}$

which is for a 20 cm long Ta-target

$$f_\ell \approx 600 \text{ Hz}$$

and which is, as expected much lower than the axial ($f_z \approx 7.8$ kHz) and in particular the radial oscillation ($f_R \approx 95$ kHz).

The lateral oscillations will lead to further loading of the material and may continue during a time over which the thermal gradient persists, which is of the order of 0.5 s.

6. Conclusion

It has been shown that with the assumed parameters and in particular with the maximum energy deposition density of 40 J/gr along the target center, a Ta-target with a diameter of 2 cm will resist to a single proton burst at room temperature. Indeed in this case the peak stresses are still below the yield strength of the material. Depending now on the cooling

of the target, its average temperature will stabilize at an elevated level and target failure is likely to occur. Moreover, at 50 Hz, which amounts to 4.3 x 10^6 pulses per day, fatigue will set in rather quickly, even when the load from each burst remains below the yield strength.

Unfortunately, it will not be possible in a neutrino factory to extend the bunch length, i.e. the heating duration to the order of μs, where stress waves in the material start to decrease. Increasing the beam and together with it the target diameter, reduces the local energy density. At best, relevant parameters, like stored kinetic energy, stresses, pressures and material velocities, scale down with $1/R^2$.

As a pessimistic assumption for liquid targets, cavitation may set in as soon as the pressure becomes negative in the target which is about 6 μs after the proton burst. Whether this starts in the center where the largest depression occurs first or close to the boundary where at moderate negative pressures the highest velocities arise, cannot be answered by this classical assessment. More sophisticated methods and computer codes will have to be applied. The strong magnetic field of 20 T of the solenoid around the target will not damp significantly the initial velocity of the target material vibrating or, in the case of cavitation, exploding in radial direction.

References :

[1] P. Drumm, C. Densham, R. Bennett, " Target Studies for the Neutrino Factory at the Rutherford Appleton Laboratory ". Contribution to Nufact'00.

[2] J. Alessi et al, " An R&D Program for Targetry and Capture at a Muon Collider Source ", proposal to the BNL AGS (Sept. 28, 1998).

[3] P. Sievers, " Elastic stress waves in matter due to rapid heating by an intense high-energy particle beam ", CERN, LAB. II /BT/74-2, June 1974.

[4] P. Sievers & P. Pugnat " Thermally induced stress waves in solid and liquid cylinders, a classical assessment ", CERN, *in preparation*, (October 2000).

Annex 1

Material Constants for Tantalum

Density:	$\rho = 16.8 \text{ x} 10^3 kg/m^3$
Young's Modulus:	$E = 16 \text{ x} 10^{10} N/m^2$
Linear Thermal Expansion Coefficient:	$\alpha_L = 6.5 \text{ x} 10^{-6} K^{-1}$
Specific Heat:	$c_V = 151 J/kg K$ (*at room temperature*)
Poisson Ratio:	$\nu = 1/3$
Velocity of Sound:	$c = \sqrt{\frac{E}{\rho} \frac{(1-\nu)}{(1+\nu)(1-2\nu)}} = 3.8 km/s$

Material Constants for Mercury

Density:	$\rho = 13.5 \text{ x} 10^3 kg/m^3$
Compressibility:	$\kappa = 0.45 \, x \, 10^{-10} m^2/N$
Volume Thermal Expansion Coefficient:	$\alpha_V = 18.1 \text{ x} 10^{-5} K^{-1}$
Specific Heat:	$c_V = 140 J/kg K$
Velocity of Sound:	$c = 1/\sqrt{\kappa\rho} = 1.3 km/s$
Electrical Conductivity:	$\varepsilon = 10^6 [\Omega m]^{-1}$

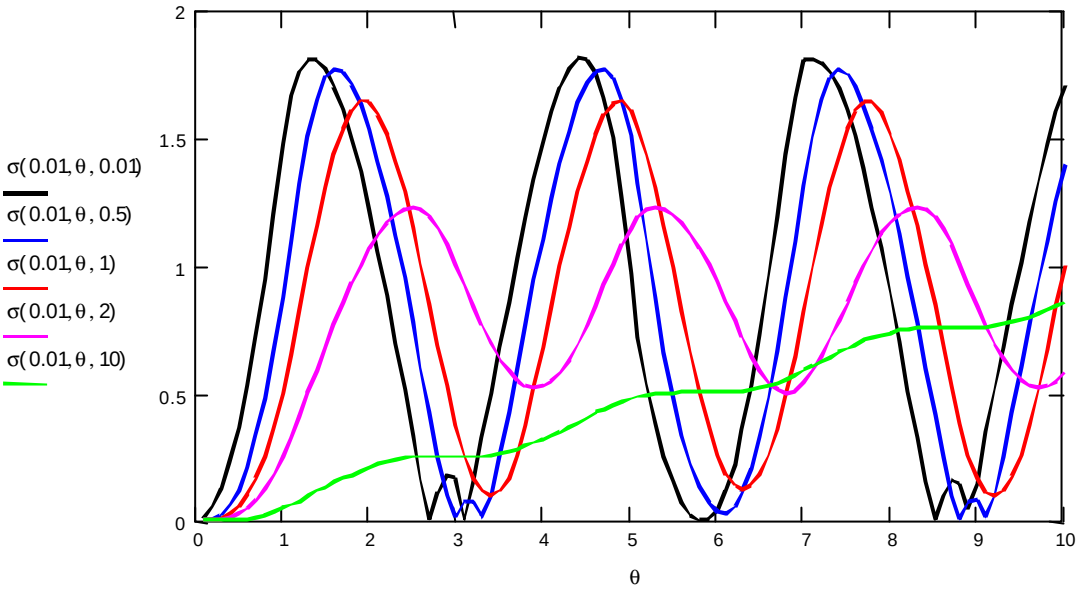

Fig. 1: Equivalent v. Mieses stress (in relative units of $Ea_L\Delta T_0$) vs. time q (q in relative units of *R/c*) in the center of a solid target. In addition to the black curve, which is for infinitely fast heating, also oscillations are shown for uniform heating over the durations $q_0 = 0.5, 1, 2$ and 10 (q_0 in units of R/c).

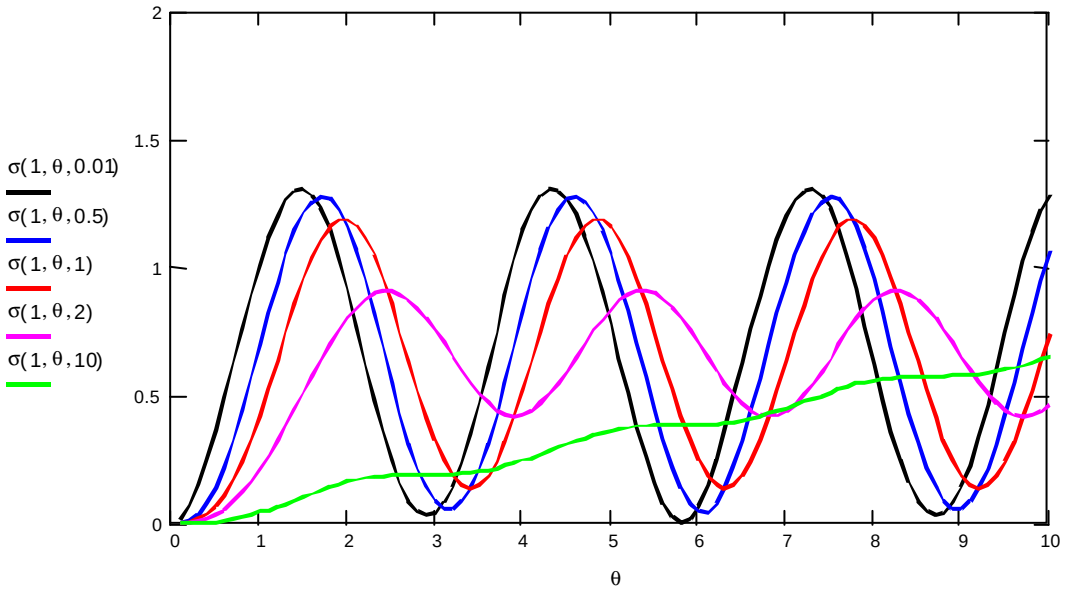

Fig. 2: Equivalent v. Mieses stress vs. time at the outer radius of a solid target. The same units as in Fig. 1 apply.

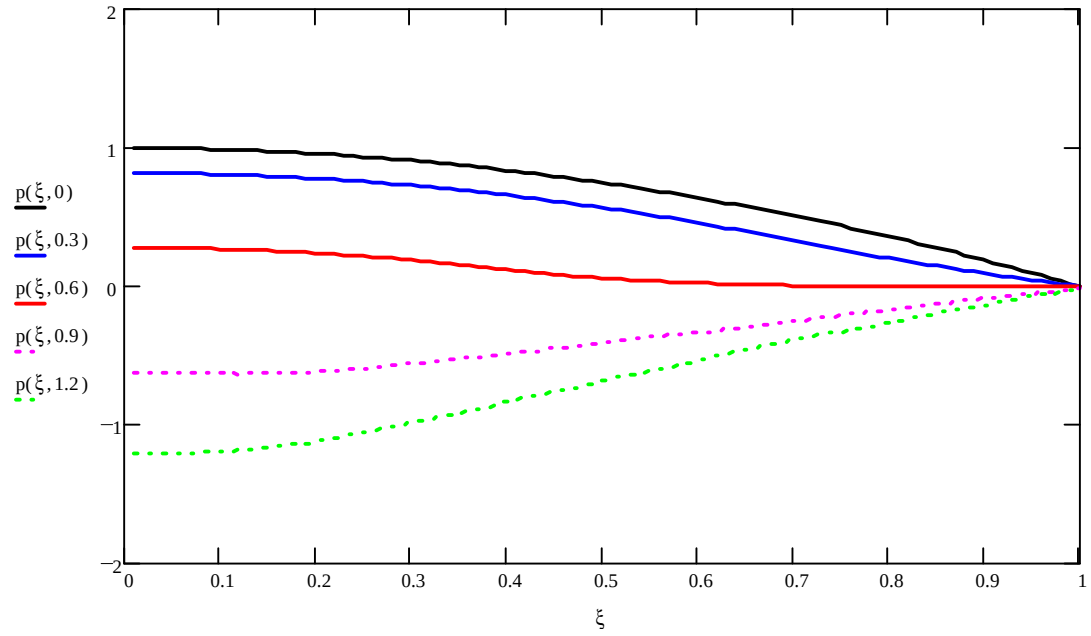

Fig. 3: Pressure (in relative units of $\alpha_V \Delta T_0 / \kappa$) vs. radial position ξ (in units of R) in a liquid target at different times θ (in relative units of R/c) of 0, 0.3, 0.6, 0.9 and 1.2.

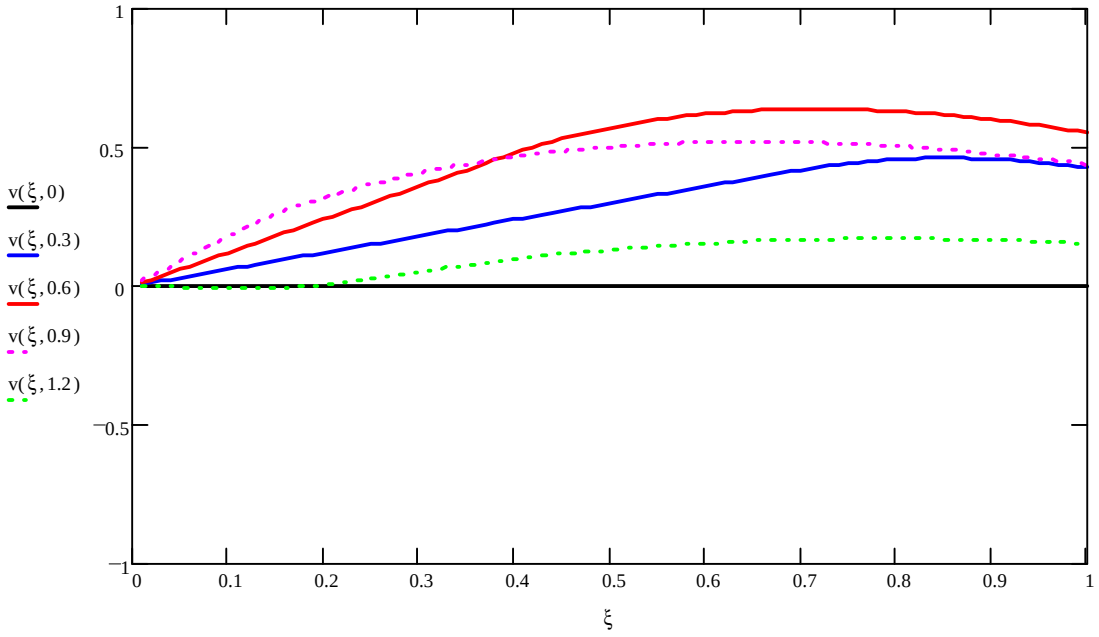

Fig. 4: Material velocity (in relative units of $\alpha_V \Delta T_0 c$) vs. radial position ξ (in units of R) in a liquid target at different times θ of 0, 0.3, 0.6, 0.9 and 1.2 (θ in units of R/c).

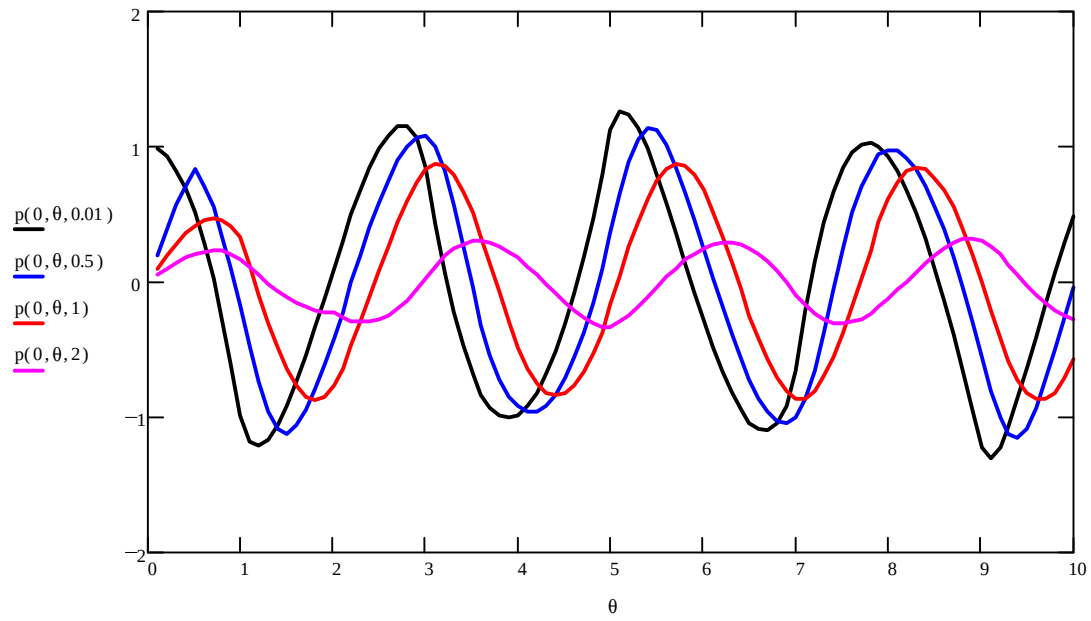

Fig. 5: Pressure (in relative units of $\alpha_V \Delta T_0 / \kappa$) vs. time θ (θ in units of *R/c*) in the center of the liquid target. In addition to infinitely fast heating with $\theta_0 = 0$, oscillations are shown for slower heating over the durations $\theta_0 = 0.5, 1 \text{ and } 2$ (in relative units of *R/c*).

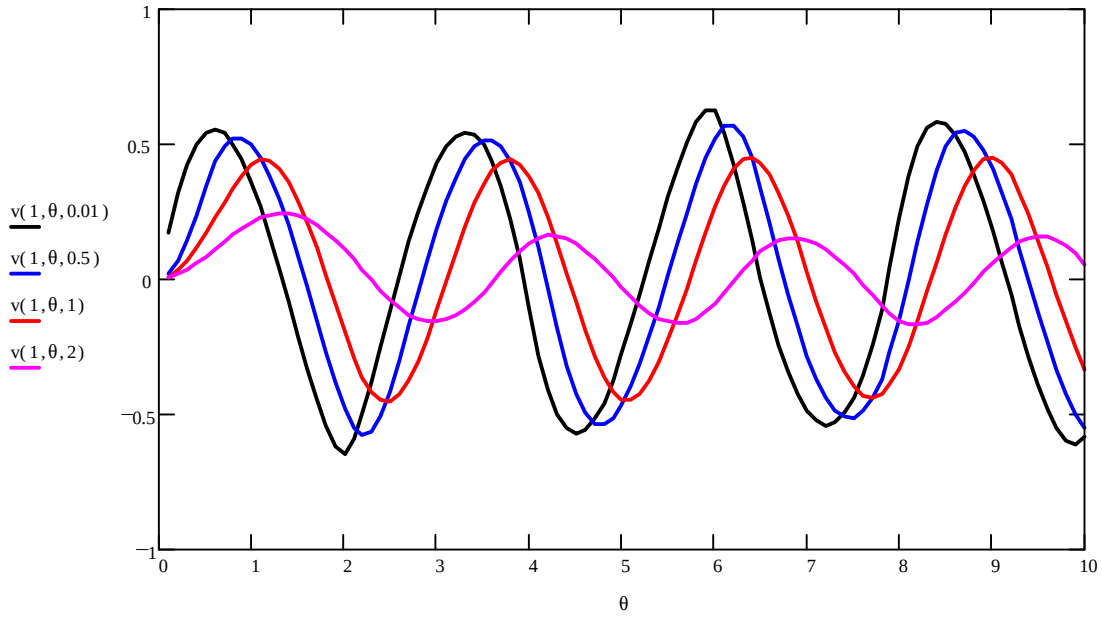

Fig. 6: Material velocity (in relative units of $\alpha_V \Delta T_0 c$) vs. time θ (in units of *R/c*) at the outer radius of the liquid target. In addition to infinitely fast heating with $\theta_0 = 0$, oscillations are shown for slower heating over the durations $\theta_0 = 0.5, 1 \text{ and } 2$ (θ_0 in units of *R/c*).